



Anti-angiogenesis therapy overcomes the innate resistance to PD-1/PD-L1 blockade in VEGFA-overexpressed mouse tumor models

Qiaohong Wang^{1,2} · Jingze Gao^{1,2} · Wen Di^{1,2} · Xia Wu^{1,2}

Received: 5 November 2019 / Accepted: 11 April 2020 / Published online: 28 April 2020
© Springer-Verlag GmbH Germany, part of Springer Nature 2020

Abstract

The effectual clinical benefits of immune checkpoint inhibitor (ICI) are hampered by a high rate of innate resistance, and VEGFA may contribute to ICI treatment resistance. In this study, we endeavored to assess the tumor microenvironment (TME) in VEGFA-overexpressed human tumors and mouse tumor models, and to explore whether anti-angiogenesis therapy can overcome the innate resistance to ICI in hyperangiogenesis mouse tumor models and the underlying mechanism. Effect of VEGFA on clinical prognosis and TME was analyzed using TCGA data. The VEGFA-overexpressed mouse breast and colon subcutaneous models were established. PD-1 mAb or apatinib alone and combination therapy were used. Immunohistochemistry and immunofluorescence were used to assess angiogenesis and hypoxia. Flow cytometry, RNA sequencing and MCP-counter were applied to detect tumor immunomicroenvironment. High level of VEGFA mRNA in human tumors is related to poor prognosis and hypoxic, angiogenic and immunosuppressive TME. Upregulation of VEGFA increased the degree of malignancy of tumor cells in vitro and in vivo. VEGFA-overexpressed models were characterized by hypoxic, hyperangiogenic and immunosuppressive TME and indicated innate resistance to ICI. In tumor-bearing mice without VEGFA overexpression, the combination therapy had no synergistic anti-tumor effect compared to monotherapy. However, apatinib alleviated hyperangiogenesis and hypoxia in TME and converted the immunosuppressive TME into an immunostimulatory one in VEGFA-overexpressed tumors. Thus, anti-angiogenesis therapy could improve the efficiency of ICI in VEGFA-overexpressed tumors. Revealing whether there is hypervascularization in tumor tissues may help to clarify the adoption of anti-angiogenesis and ICI combination therapy or ICI monotherapy in cancer treatment.

Keywords Innate resistance to PD-1/PD-L1 blockade · Hyperangiogenesis · Hypoxia · Apatinib · Tumor immune microenvironment

Abbreviations

AA Anti-angiogenesis
GSEA Gene set enrichment analysis
ICI Immune checkpoint inhibitor

ICER Incremental cost-effectiveness ratio
IPRES Innate anti-PD-1 resistance
KI Tyrosine kinase inhibitor
LAG-3 Lymphocyte activation gene-3
MDSCs Myeloid-derived suppressor cells
MVD Microvascular density
ORR Objective response rates
OS Overall survival
PD-1 Programmed cell death 1
PD-L1 Programmed cell death ligand 1
QALY Quality-adjusted life-year
RCC Renal cell carcinoma
TCGA The Cancer Genome Atlas database
TIGIT T cell immunoreceptor with Ig and ITIM domain
TILs Tumor-infiltrating lymphocytes
TIM-3 T cell immunoglobulin and mucin-domain containing-3

Qiaohong Wang and Jingze Gao are contribution equally to this work.

Electronic supplementary material The online version of this article (<https://doi.org/10.1007/s00262-020-02576-x>) contains supplementary material, which is available to authorized users.

✉ Xia Wu
wuxia1225@aliyun.com

¹ Department of Obstetrics and Gynecology, School of Medicine, Renji Hospital, Shanghai Jiaotong University, Shanghai 200127, People's Republic of China

² Shanghai Key Laboratory of Gynecologic Oncology, Shanghai 200127, People's Republic of China

TME	Tumor microenvironment
TOX	Thymocyte selection-associated HMG box protein
Tregs	T regulatory cells
TRAE	Treatment-related adverse effect
UCSC	University of California Santa Cruz database
VEGFA	Vascular endothelial growth factor A

Introduction

Immune checkpoint inhibitor (ICI) therapy, through the inhibition of the interaction between programmed death-1 (PD-1), mostly expressed on activated CD8⁺ T cells [1], and its ligand PD-L1, has represented a tremendous revolution in the treatment for various malignancies [2, 3]. PD-1/PD-L1 blockade could re-invigorate the impaired T cells and restore the cytotoxic activity against tumor cells [4, 5]. However, the efficacy of monotherapy PD-1/PD-L1 blockade was only 20–40% in most cancer types, and there are a large number of partial responders [5, 6]. Quite a few patients do not respond to PD-1/PD-L1 blockade initially, recognized as "primary resistance (innate resistance)," as mentioned in our review [7]. Roger et al. [8] revealed that the tumor microenvironment (TME) of hyperangiogenesis is closely related to the intrinsic resistance to PD-1/PD-L1 blockade. Through whole exome sequencing and gene set enrichment between the responding versus nonresponding pretreatment tumors from malignant melanoma patients treated with PD-1 mAb, a group of 26 transcriptomic signatures were defined in nonresponding tumors. The special transcriptomic profile involved in hypoxia, pro-angiogenesis, epithelial–mesenchymal transition and wound healing is named the Innate anti-PD-1 Resistance (IPRES) signature, among which high expression of vascular endothelial growth factor A (VEGFA) is the key element [8].

VEGFA has a pivotal role in promotion of tumor angiogenesis. Angiogenesis, the formation of a tumor-associated vascular network, is crucial for tumor growth and progression. Abnormal tumor vasculature often interferes with drug penetration in tumor areas and generates a hypoxic and acidic TME [9–11]. Hypoxia further promotes angiogenesis, epithelial–mesenchymal transition and tumor metastasis and aggravates hypoxia and immunosuppression through hypoxia-inducible factor 1 (HIF-1), forming a vicious circle in TME [12]. VEGFA, or hypoxia and hyperangiogenesis, has notable influence on anti-tumor immunity, mainly relying on promotion of inhibitory immune cell populations [13–18], affection of effector T cell response and alteration of lymphocyte development and trafficking [19, 20]. Effective anti-tumor response of PD-1/PD-L1 blockade mainly depends on the ability of specific T cells to infiltrate into tumors, but patients with hypoxic, hyperangiogenic and

immunosuppressive TME are less likely to benefit from the therapy. VEGFA, the key element in IPRES transcriptomic signature, was found to be correlated with innate anti-PD-1 resistance by other researchers. Chen et al. [21] suggested a VEGFA-related mechanism of therapeutic resistance according to the increased expression of VEGFA gene in nonresponding metastatic melanoma patients treated with PD-1 mAb. Emerging data suggest that anti-angiogenesis (AA) may exert positive immunomodulatory activity in the immunosuppressive TME. AA and ICI combination therapy may have a synergistic effect, since complementary mechanisms exist between the AA and ICI. Retrospective and clinical studies have demonstrated that patients receiving AA agents and ICI have longer overall survival (OS) than the monotherapy in some clinical settings [22–25]. In CheckMate 016 study, which compared the safety and efficacy of nivolumab combined with sunitinib or pazopanib in patients with advanced or metastatic renal cell carcinoma (RCC), objective response rates (ORR) were 55% and 45%, respectively [26]. In a phase II study, the ORR of lenvatinib and pembrolizumab was 39.6% in advanced endometrial cancers [27]. In the IMmotion 151 trial, 37% of patients who received atezolizumab plus bevacizumab have achieved a confirmed objective response in RCC [25]. Apart from the encouraging antitumor effect, however, most combination therapy had a tolerable but really high incidence of serious adverse events about 32–82% [22, 24–28]. Considering the higher toxicity and cost of AA and ICI combination therapy, it is still not known whether combination therapy has more benefits than monotherapy for all patient including those without hypoxic and hyperangiogenic TME. There is an urgent need to make the best use of AA and ICI combination therapy and explore the most appropriate patients according to the characteristics of TME or other biomarkers.

Apatinib is an oral small-molecule VEGFR-2 tyrosine kinase inhibitor (TKI) that highly and selectively blocks VEGFR-2, inhibiting VEGFA-mediated endothelial cell proliferation and migration [29]. VEGFR-2 is recognized as the main receptor conveying the proangiogenic signals downstream of VEGFA. Up to date, lots of studies have shown the promising therapeutic effect of apatinib in multiple solid tumors [30–35]. The convenient administration and lower financial burden than anti-VEGF or anti-VEGFR2 anti-bodies or other VEGFR TKIs make apatinib a meaningful and emerging anti-angiogenesis therapy. In this study, we assessed the characteristics of TME in VEGFA-overexpressed human tumors and mouse tumor models. The anti-tumor effects of PD-1 mAb or apatinib alone and the combination therapy were assessed in VEGFA-overexpressed or normal mouse models. The underlined mechanisms for the very likely synergistic effect of ICI and AA combination therapy in VEGFA-overexpressed mouse models were also explored. This study tries to reverse innate resistance

to PD-1/PD-L1 blockade therapy in tumors with hyperangiogenic and hypoxic TME, which may help to make the best use of AA and ICI combination therapy for appropriate patients in cancer treatment.

Methods

Analysis of the effect of VEGFA on clinical prognosis and TME

Patients were quarter divided into four groups according to the expression of VEGFA, with data from the Cancer Genome Atlas (TCGA) database processed by UCSC Xena platform (<https://xenabrowser.net/datapages/>), which the top 25% patients and the bottom 25% patients were selected as VEGFA-high and VEGFA-low. Kaplan–Meier survival analysis of OS in pan-cancer, colon and breast cancer was performed according to the VEGFA expression in R. Gene set enrichment analysis (GSEA) 2.2.4 software was downloaded and used to assess the difference of the set genetic signatures between VEGFA-high and VEGFA-low. Whole gene expression matrix was used as the input gene matrix, and expression of VEGFA was used as the input biomarker. Immune cell types could be quantified by gene signature set expression using machine calculation methods [36]. We used the immune cell markers established by Bindea et al. [36] to quantify the amounts of tumor-infiltrating immune cells and explore the relationship between VEGFA and immune cells by R GSVA package. Spearman correlation coefficients (r_{Pearson}) and corresponding p values were used to depict the correlation on the scatter plots.

Tumor cell lines

The murine colon carcinoma cell line CT26 and mammary cancer cell line 4T1 were both purchased from the Cell Bank of the Chinese Academy of Sciences (Shanghai, China). The cells were maintained in RPMI-1640 (Hyclone, USA) supplemented with 10% fetal bovine serum (FBS) (Gibco, USA) and 1% penicillin–streptomycin (Gibco) and cultured in a 37 °C incubator with a humidified atmosphere containing 5% CO₂.

Lentiviral infections

The lentivirus of control and overexpression VEGFA was purchased from OBiO Technology Corp., Ltd. (Shanghai, China). CT26 and 4T1 cells were infected with lentivirus supernatant fluid in medium containing 5 µg/ml polybrene. Stable transfected CT26 and 4T1 cells were selected by puromycin with final concentrations of 1 µg/ml and 8 µg/

ml (Sigma, USA), respectively, and verified by quantitative real-time PCR and Western blot.

Quantitative real-time PCR

Total RNA was extracted using trizol (Invitrogen, USA), and cDNA was synthesized using the Reverse Transcriptase M-MLV kit (Takara, Japan) according to manufacturer's instructions. Quantitative real-time PCR analyses were performed with specific primers using SYBR Green PCR Master Mix (Takara). The primers for VEGFA were 5'-ACG ACAGAAGGAGAGCAGAAG-3' and 5'-ACACAGGAC GGCTTGAAGAT-3'. Glyceraldehyde-3-phosphate dehydrogenase (GAPDH) was used as a reference gene.

Western blot analysis

Cells were lysed with RIPA buffer, and acquired protein was separated by 10% SDS-PAGE gel electrophoresis. Then, the separated protein was transferred onto a PVDF membrane blocked with 5% skim milk for 1 h. 87u9tt6u9tt6The primary antibody (Ab) was VEGFA (ab1316, Abcam, USA), and secondary antibody was HRP-labeled goat-anti-mouse IgG. GAPDH was served as the internal control.

Colony formation assay

The cells were maintained in complete medium and seeded in a 6-well plate with 200 cells/well for two weeks to allow colony formation. The visible colonies were then fixed in paraformaldehyde and stained with crystal violet (Sigma) for counting.

Cell proliferation assay (CCK-8 assay)

Cells in exponential growth were plated in a 96-well plate with 3×10^3 cells/well for different culture times. Each well was replaced with 100 µL of RPMI-1640 medium containing 10 µL of CCK-8 and incubated for 40 min before testing. Optical density (OD) of each well was measured at 450 nm by a microplate reader (Thermo Scientific, USA).

Cell cycle analysis

For cell cycle analysis, cells were cultured for 72 h. Then, each sample was collected and fixed using ice-cold 75% ethanol. PI/RNase staining solution (BD Biosciences, USA) was added to the cells for 30 min. Flow cytometric analysis (NovoCyte, Agilent, USA) was used to analyze cell cycle distribution.

Migration and invasion assay

Cell migration and invasion assays were performed using 24-well plates and 8 μm chambers (Corning, USA). For the migration assay, 3×10^4 CT26-VEGFA or CT26-control cells and 5×10^4 4T1-VEGFA or 4T1-control cells were plated in each upper chamber. For the invasion assay, the upper chamber was coated with Matrigel (BD). The cells of CT26-VEGFA or CT26-control in each chamber were 8×10^4 , and those of 4T1-VEGFA or 4T1-control were 1×10^5 . In both assays, there was serum-free medium in upper chamber while medium contains 10% FBS in lower chamber. After incubating for 24 h, the migrant cells were fixed with 4% paraformaldehyde, stained with 0.1% crystal violet and counted in five random fields at 400 \times magnification. Each experiment was conducted in triplicate.

Animals and tumor models

Eighty BALB/c mice (aged 5–6 weeks, female) were kept under specific pathogen-free (SPF) conditions. All the mice were subcutaneously implanted tumor cells in the right flank, and the day of the inoculation was recorded as day 0. For CT26 model, 1×10^5 cells of CT26-control and CT26-VEGFA in 100 μL PBS were injected. And 4T1-control and 4T1-VEGFA cells were injected at 5×10^5 cells in 100 μL PBS for 4T1 group. Cells of control and VEGFA overexpression were stably transfected with luciferase (Luc) gene. Tumor volumes were measured with calipers and calculated according to the following formula: Tumor Volume (mm^3) = Length (mm) \times Width (mm)²/2. Once the tumor volume reaches 50–100 mm^3 (about day 7), the mice in both CT26 and 4T1 groups were randomly divided into eight subgroups ($n = 5$ for each group) and received different treatments. Apatinib (Jiangsu Hengrui Medicine Co., Ltd, China) was diluted in 0.5% (w/v) carboxymethyl cellulose and administered once daily through intragastric administration (ig) for two weeks (100 mg/kg). Anti-PD-1 antibody (Rat IgG2a, Clone RMP1-14, Bio X Cell, USA) was injected intraperitoneally (i.p.) every three days in two weeks (~ 10 mg/kg). Tumor volume and mouse bodyweight were monitored twice every week. All mice were anesthetized and injected (i.p.) with 3 mg/200 mL D-luciferin (GoldBio Technology, USA) at the end of the treatment to capture bioluminescence images using an IVIS Spectrum (Xenogen, USA). The mice were euthanized on day 23. All animal experiments were performed according to protocols approved by Renji Hospital, School of Medicine, Shanghai Jiao Tong University.

Immunohistochemistry and immunofluorescence of the tumors

Tumors were collected, fixed and paraffin-embedded to perform IHC and IF staining. The sections were incubated with anti-VEGFA (1:500, Abcam) (red), anti-CD31 (1:100, Cell Signal Technology, USA) and anti-HIF-1 α (1:100, Santa Cruz, USA) (Green) antibodies overnight, followed by incubation with HRP- or fluorescence-labeled secondary antibodies. Nuclei were counterstained with hematoxylin in IHC and with DAPI according to IF (Sigma).

RNA sequencing and analysis

Tumors in different groups were treated with trizol (Invitrogen), and total RNA was extracted using RNeasy Plus Mini Kit (Qiagen, German) according to the manufacturer's protocol. Sequencing libraries were generated using an Illumina Standard library preparation kit (Illumina, USA). After the assessment of RNA quality using an Agilent 2100 Bioanalyzer, mRNA expression levels were sequenced on the Illumina HiSeqTM 2500 platform by OE Biotech Co., Ltd (Shanghai, China). Anti-tumor immunity was evaluated by the Microenvironment Cell Population-counter (MCP-counter) method [37].

Flow cytometry

Solid tumors of mice were collected for flow cytometric analysis. Tumor-derived single-cell suspensions were obtained through the following steps: first mechanical dissociation of the gentle MACS Dissociator (Miltenyi Biotec, USA) and the incubation at 37 $^{\circ}\text{C}$ in RPMI-1640 containing Collagenase IV (2 mg/ml, Sigma), DNase I (0.02 mg/ml, Sigma) and HAase (0.1 mg/ml, Sigma), then passing through a 40- μm cell strainer (Corning) and the red blood cells removed with RBC Lysis Buffer (Sigma), followed by density gradient centrifugation at last. The cells were stained for surface markers CD45-APC-cy7 (BD), CD3-FITC (Biolegend, USA), CD4-BV510 (BD), CD8-Percp cy5.5 (Biolegend), CD11b-PE-cy7 (BD), Gr-1-BV605 (BD), F4/80-BV421 (BD), PD-1 (Biolegend), TIM-3 (BD), LAG-3 (Biolegend), TIGIT (Biolegend) at 4 $^{\circ}\text{C}$ for 30 min. And Foxp3-PE (eBioscience, USA), CD206-APC (BD) and TOX (eBioscience) were used for intracellular staining at 4 $^{\circ}\text{C}$ for 50 min. All samples were analyzed on Fortessa (BD), and the acquired data were further analyzed using Flowjo (Tree Star).

Statistical analysis

The data were expressed as the mean \pm standard deviation (SD). The differences between two groups were

analyzed using the double-sided Student's *t* test. The data were analyzed with Prism 7.0 software (GraphPad, USA) and R (3.5.1), and $P < 0.05$ was considered as statistically significant.

Results

Clinical impacts of VEGFA on prognosis and TME

First, we studied the clinical impact of VEGFA with the data from TCGA database. The survival was compared between the VEGFA-high and VEGFA-low groups through analysis of 10,531 samples across 33 tumor types. Negative correlation was found between the expression of VEGFA mRNA and OS. (Fig. 1a). There was an analogous negative correlation between colon adenocarcinoma ($n = 289$) and breast cancer ($n = 1092$) (Fig. 1b, d). Patients with microsatellite stable (MSS) tumors ($n = 174$) were negatively and significantly correlated with VEGFA mRNA expression, while those with microsatellite instable (MSI) tumors ($n = 98$) were not in colon adenocarcinoma (Fig. 1c). Further analysis indicated that high expression of VEGFA is greatly related to the enrichment of angiogenesis- and hypoxia-related genes via GSEA (Fig. 1 g, h). In-depth research of the gene data revealed an obvious correlation between the VEGFA mRNA expression and certain immune subtypes (Fig. 1 e–f). The following immune subtypes were all negatively related to the expression of VEGFA (Fig. 1 i, j), such as T cells, cytotoxic cells, etc., suggesting an inhibitory TME in colon and breast cancers with high expression of VEGFA.

The effects of VEGFA overexpression on murine tumor cells in vitro and in vivo

As patients with VEGFA-high tumors were remarkably correlated with poor prognosis, we established CT26-VEGFA and 4T1-VEGFA cell lines in which VEGFA were stably upregulated using the lentivirus. Meanwhile, as control cell lines, CT26-NC and 4T1-NC were generated with an empty vector. The upregulation of VEGFA was verified by quantitative real-time PCR and Western blot (Fig. 2a, b and Supplementary Fig. 1). We then investigated the effects of VEGFA overexpression in vitro. The cell growth curve demonstrated that VEGFA overexpression significantly enhanced cell proliferation (Fig. 2c). Meanwhile, in contrast to cells containing empty vector, the colony-forming efficiency was notably increased in CT26-VEGFA and 4T1-VEGFA cells (Fig. 2d). A conspicuous increase in the S phase in VEGFA-upregulated cells was observed through the analysis of cell cycle distribution (Fig. 2e). In addition, VEGFA overexpression markedly raised the capability of cell migration and invasion in CT26 and 4T1 cells (Fig. 2f–g).

Furthermore, we explored *in vivo* effects of VEGFA overexpression in the homograft tumor models using BALB/c mice. As is previously mentioned, CT26 and 4T1 are murine tumor cells derived from BALB/c mice [38, 39]. Tumors in CT26-VEGFA groups, where the weight was 4926.0 ± 1589.0 mg, grow far more rapidly than in CT26-NC group, where the weight was 2953.0 ± 695.0 mg. Similarly, tumor growth of 4T1-VEGFA was evidently increased compared with that of 4T1-NC (tumor weight: 2493.0 ± 324.4 mg vs. 1940.0 ± 408 mg) (Fig. 3a). Therefore, upregulation of VEGFA gene in both CT26 and 4T1 tumor cells could not only significantly enhance cell proliferation, migration and invasion in vitro, but also notably promote tumor growth in vivo.

Simultaneously, immunohistochemistry was performed to examine the influence of increased VEGFA expression on angiogenesis. VEGFA, CD31 and HIF-1 α were highly expressed in VEGFA-overexpressed tumors (Fig. 3b). Increased VEGFA expression promoted angiogenic function and formed a vicious circle in TME. Increased abnormal tumor vasculature, along with severe hypoxia, illustrated a poor condition of notably hyperangiogenic and extremely hypoxic TME. Immune microenvironment in tumor was also explored through flow cytometry. The proportion of CD8⁺ T lymphocytes was significantly declined in CT26-VEGFA (33.06 ± 3.11 vs. 26.44 ± 1.64 , Fig. 3c) and 4T1-VEGFA (23.94 ± 1.93 vs. 20.48 ± 1.72 , Fig. 3d) tumors, which seriously affected its anti-tumor immunity as a crucial member of tumor-specific killer. The proportion of inhibitory immune components, such as CD4⁺FOXP3⁺ Tregs, M2-like macrophages and myeloid-derived suppressor cells (MDSCs), appeared to be significantly elevated (Fig. 3c, d). Additionally, T exhausted cells, regarded as T cells with impaired effector capacity, often induce tumor progression. Thymocyte selection-associated HMG box protein (TOX) was identified to program and characterize CD8⁺ T cell exhaustion [40, 41]. It is reported that VEGFA has direct effect on T cell exhaustion [42]. Accordingly, we examined the exhaustion status of T cells in VEGFA-overexpressed tumors. TOX was significantly up-regulated in CD8⁺ tumor-infiltrating lymphocytes (TILs) in VEGFA-overexpressed tumors (Fig. 3e). Exhausted T cells also express multiple immune checkpoint receptors [3]. The expression of inhibitory receptors, PD-1, T cell immunoglobulin and mucin-domain containing-3 (TIM-3), lymphocyte activation gene-3 (LAG-3) and T cell immunoreceptor with Ig and ITIM domain (TIGIT) on CD8⁺ TILs was notably elevated (Fig. 3f, g). Together, we deduced a landscape of a hyperangiogenic, hypoxic and especially immunosuppressive TME in VEGFA-overexpressed tumors, which is of highly possibility to generate innate nonresponse to PD-1/PD-L1 blockade.

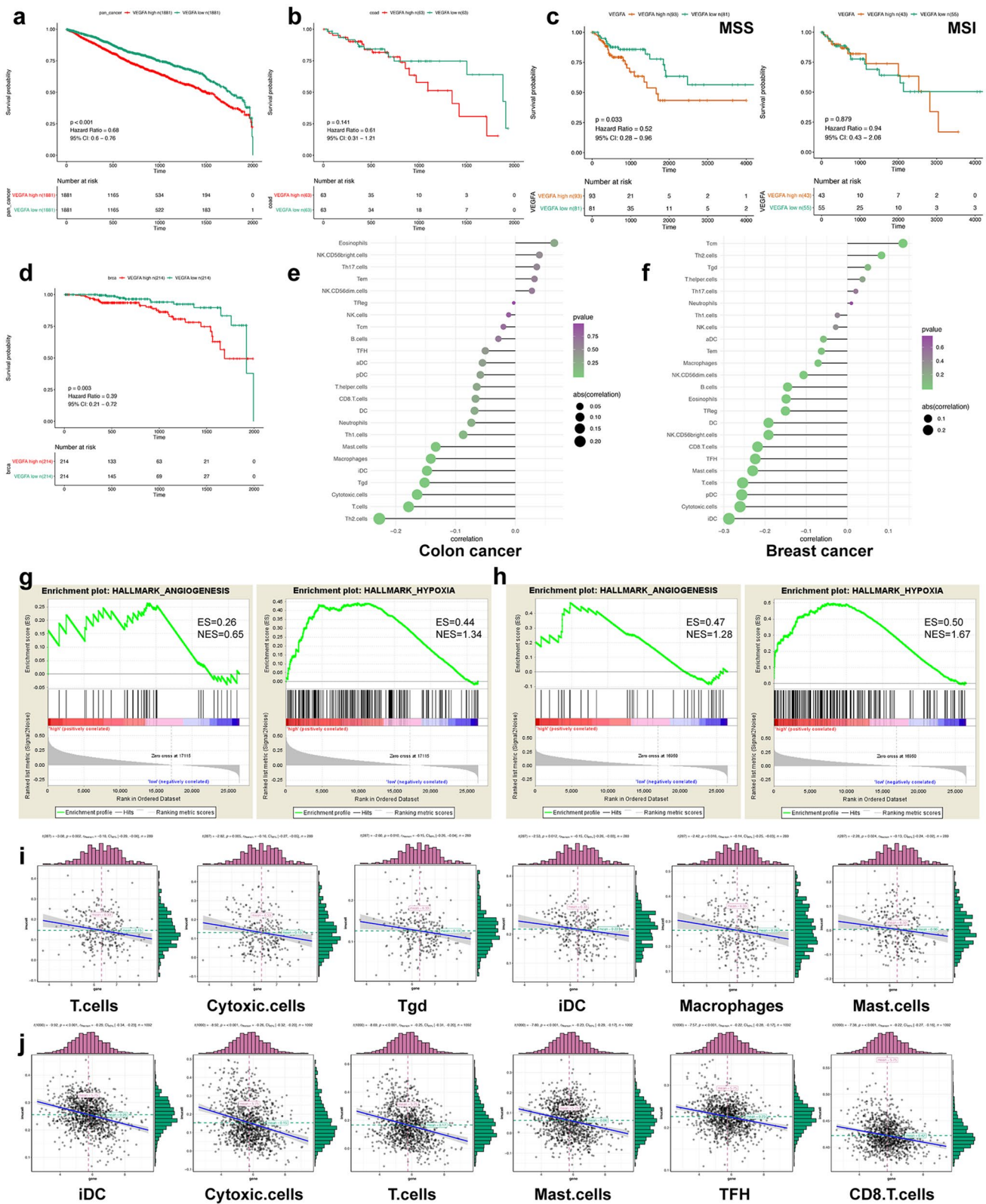


Fig. 1 High expression of VEGFA is related to poor prognosis and hypoxic, angiogenic and immunosuppressive TME. Survival analysis in pan-cancer (a), colon adenocarcinoma (b), MSS and MSI colon adenocarcinoma (c) and breast cancer (d). Gene set enrichment analysis

showed that VEGFA high expression is highly related to the enrichment of angiogenesis- and hypoxia-related genes (g–h). Negative correlation was found between high expression of VEGFA and immune cells in colon (e and i) and breast cancer (f and j), respectively

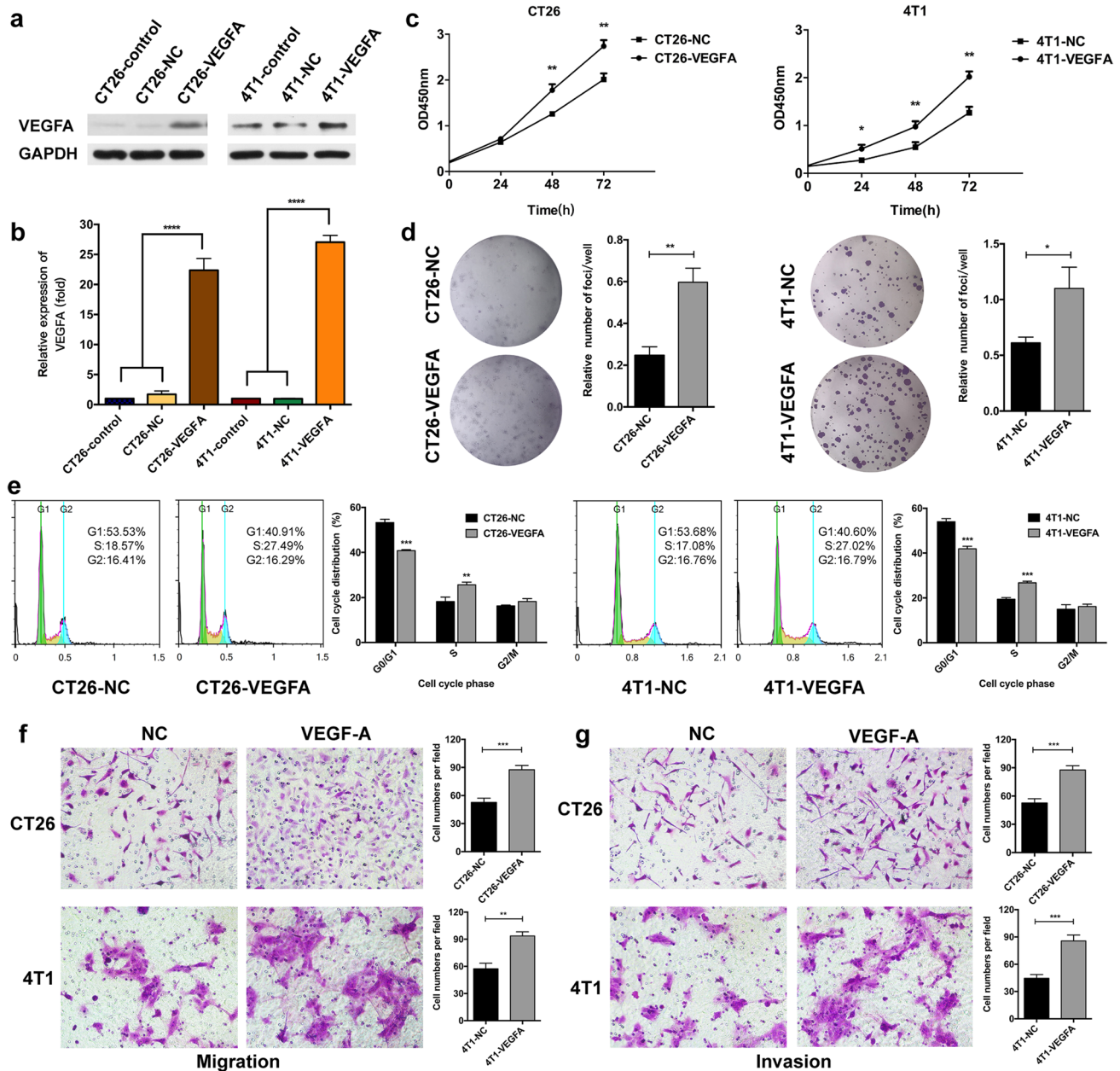


Fig. 2 Effects of VEGFA overexpression on murine tumor cells in vitro. The upregulation of VEGFA in CT26 and 4T1 cells, using VEGFA-Luc lentivirus (a–b), **** $p < 0.0001$. Increased proliferation in CT26-VEGFA and 4T1-VEGFA cells was confirmed by CCK-8 assay and colony formation assay (c–d), ** $p < 0.01$, * $p < 0.05$. The cell cycle was assessed using flow cytometry analysis

in tumor cells with or without VEGFA expression (e), *** $p < 0.001$. Transwell assays were performed to detect the effect of VEGFA overexpression on cell migration (f) and invasion (g), *** $p < 0.001$, ** $p < 0.01$. -VEGFA: the group of mice bearing VEGFA-overexpressed tumor cells, -NC: the group of mice bearing tumor cells with empty vector

Resistance to PD-1/PD-L1 blockade was observed in VEGFA-overexpressed mouse models

Considering the pivotal role of VEGFA in pro-angiogenesis and drug resistance among IPRES transcriptional signature, we attempted to establish a PD-1 monoclonal antibody (mAb)-resistant model to investigate the effect of VEGFA

overexpression on drug resistance using normal BALB/c mice. CT26-VEGFA and CT26-NC tumors were given apatinib or PD-1 mAb alone and in combination, respectively, and PBS was used as control. Same regimen was administrated in 4T1 mouse tumors. As in CT26-NC group, the anti-tumor effect of PD-1 mAb monotherapy was significantly higher than that of control group (Fig. 4a–d and Supplementary Fig. 2a, c).

Tumor weight was 1477.0 ± 723.8 mg for the group receiving PD-1 mAb, whereas tumor weight was 2953.0 ± 695.0 mg in control group (Fig. 4d). However, it is observed that PD-1 mAb had no significant anti-tumor effect on VEGFA-overexpressed tumors, where tumor weight was 4192.0 ± 2200.0 mg in PD-1 mAb monotherapy group and 4926.0 ± 1589.0 mg in control group (Fig. 4d). Likewise, analogous results were found in 4T1 mouse tumor models (Fig. 4e–h Supplementary Fig. 2a, c). The little anti-tumor response of PD-1 mAb in

Fig. 4 Anticancer effect in subcutaneous colon and breast cancer model. Fluorescent images of mice at the end of the treatment (a and e). Photographs of the subcutaneous tumors three days after the end of the treatment (b and f). Tumor growth curve of mice receiving i.p. injection of anti-PD-1 antibody at a dose of 10 mg/kg every 3 days alone and corresponding to 100 mg apatinib per kg body weight daily, in both -NC and -VEGFA tumors (c and g). Weight comparison of the subcutaneous tumors in different treatment groups (d and h). **** $p < 0.0001$, *** $p < 0.001$, ** $p < 0.01$, * $p < 0.05$. -VEGFA: the group of mice bearing VEGFA-overexpressed tumor cells, -NC: the group of mice bearing tumor cells with empty vector

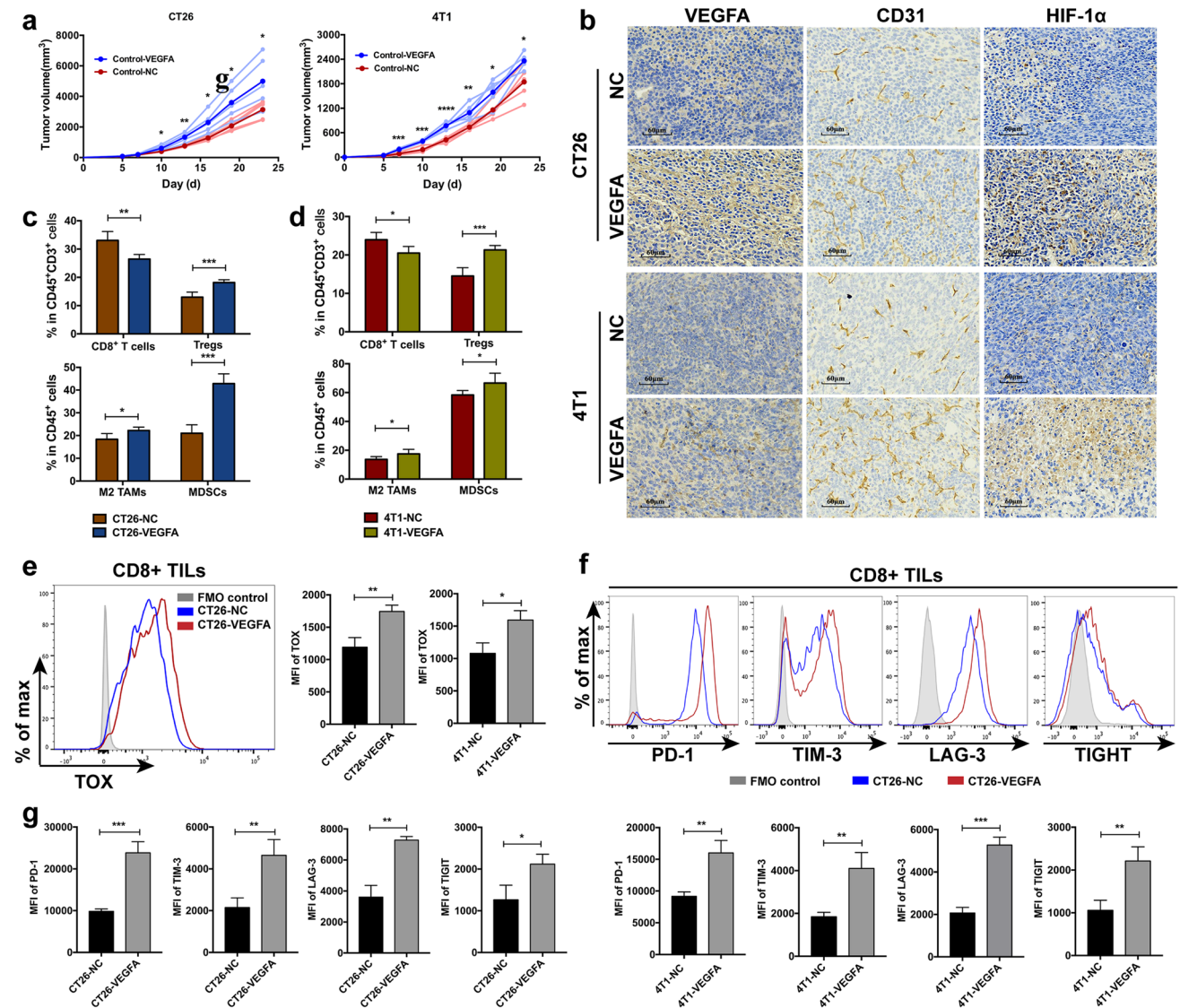
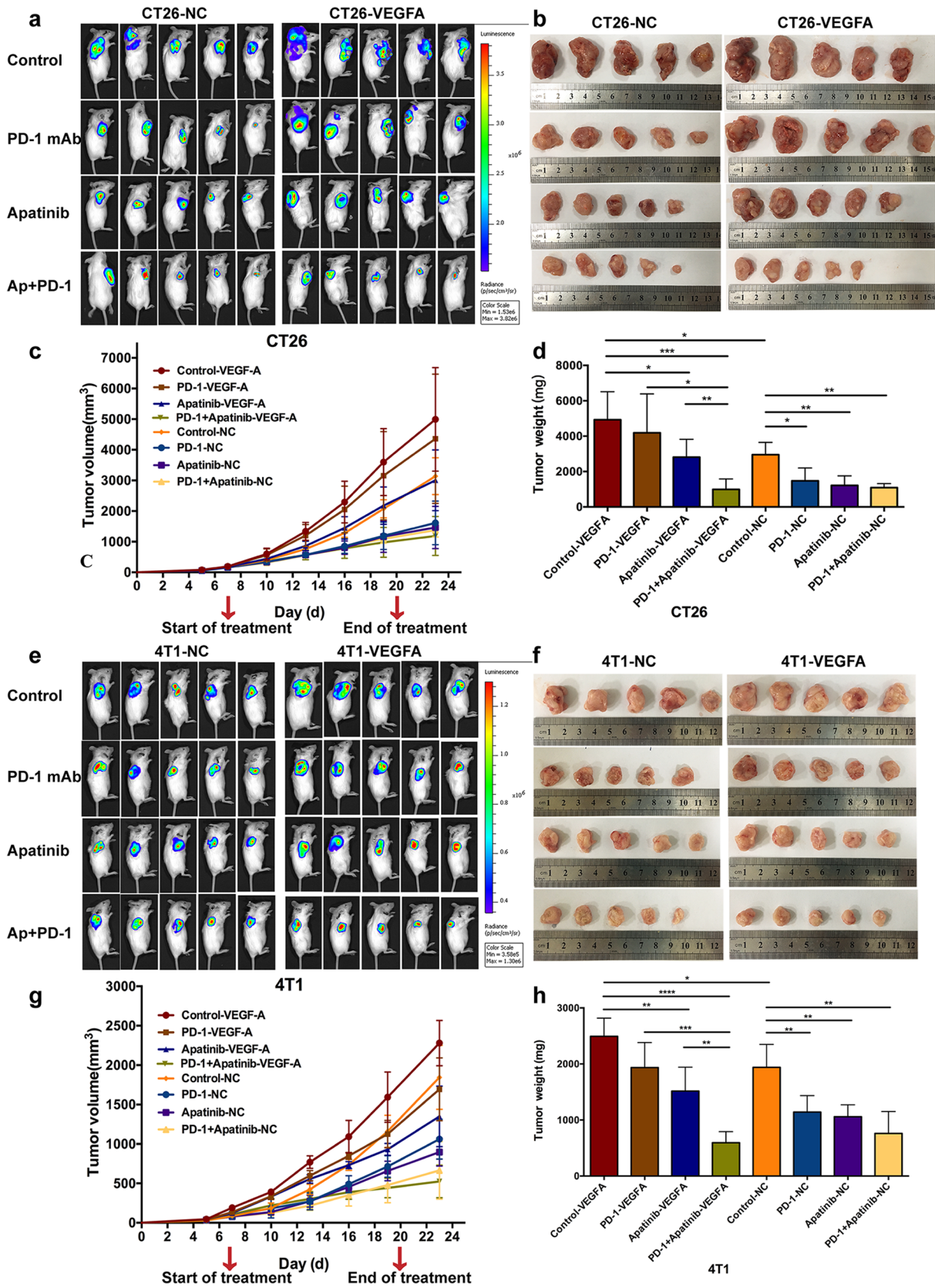


Fig. 3 Effects of VEGFA-overexpression on murine tumor cells in vivo. Tumor volume curve showed enhanced tumor growth in mice with VEGFA-overexpression colon and breast cancer cells (a). Tumor angiogenesis (b) and immune (c–d) microenvironment deteriorated due to the overexpression of VEGFA. **** $p < 0.0001$, *** $p < 0.001$, ** $p < 0.01$, * $p < 0.05$. Upregulated expression of

TOX among CD8⁺ T cells in -VEGFA tumors (e), ** $p < 0.01$, * $p < 0.05$. Elevated levels of inhibitory receptors on CD8⁺ T cells in -VEGFA tumors (f and g), such as PD-1, TIM-3, LAF-3, and TIGIT, *** $p < 0.001$, ** $p < 0.01$, * $p < 0.05$. -VEGFA: the group of mice bearing VEGFA-overexpressed tumor cells, -NC: the group of mice bearing tumor cells with empty vector



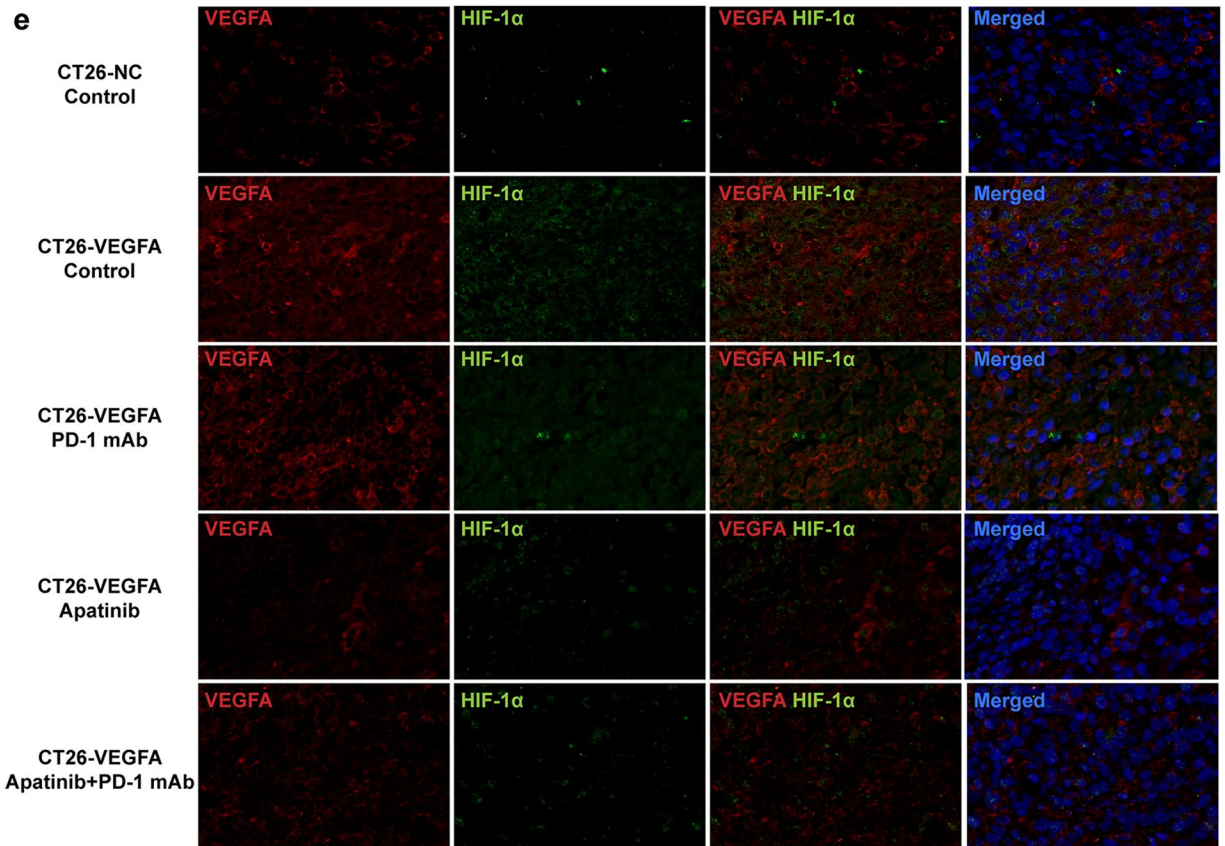
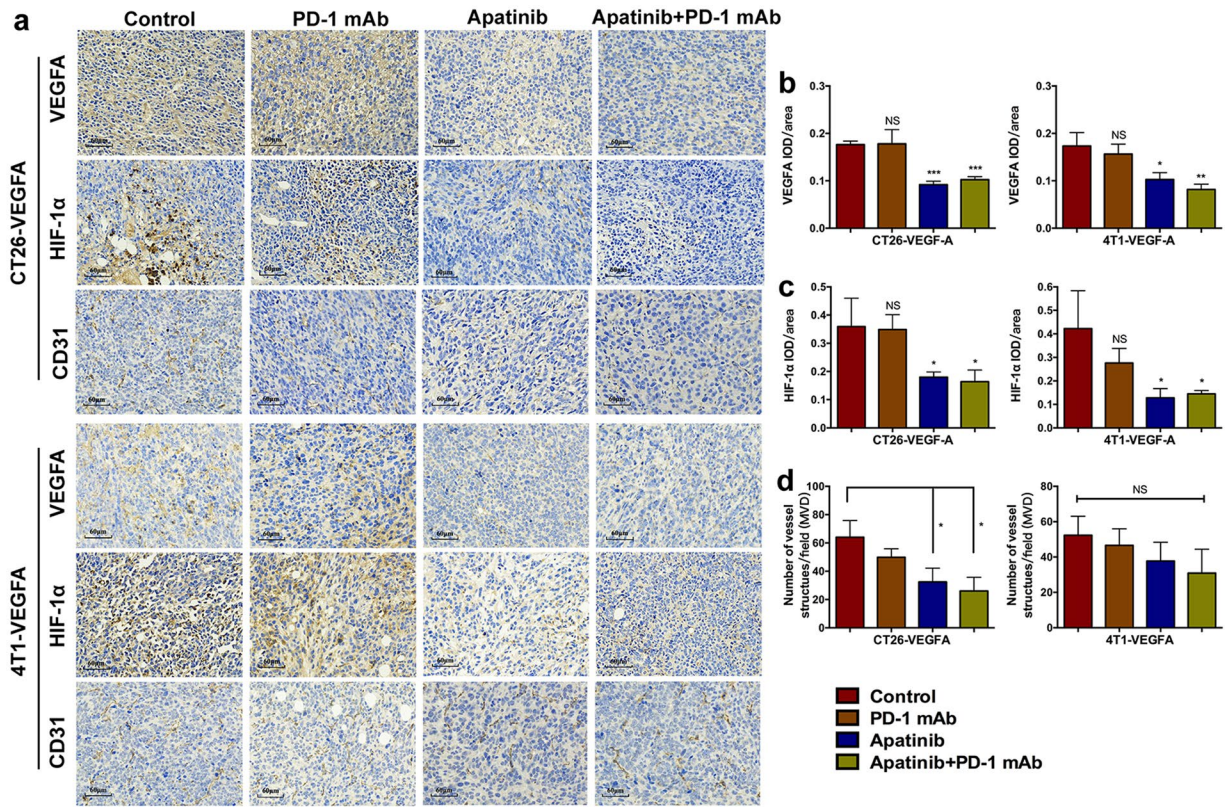


Fig. 5 Combining apatinib with PD-1 mAb improved the hyperfunction of angiogenesis and hypoxia. Immunohistochemistry detecting the expression of VEGFA, HIF-1 α and CD31 in hyperangiogenic tumors receiving different treatments (a). The immunohistochemical staining analysis of VEGFA (b), HIF-1 α (c) and CD31 (d) in VEGFA-overexpressed mouse models, *** $p < 0.001$, ** $p < 0.01$, * $p < 0.05$. Double-labeled immunofluorescent staining of VEGFA (red) and HIF-1 α (green) in CT26 tumors (e). -VEGFA: the group of mice bearing VEGFA-overexpressed tumor cells, -NC: the group of mice bearing tumor cells with empty vector

VEGFA-overexpressed tumors was consistent with the hyperangiogenic, hypoxic and immunosuppressive TME, which may be responsible for the nonreaction. Hence, tumors which received injection of VEGFA-overexpressed cells hardly ever responded to PD-1 mAb monotherapy, thus identifying an innate resistant tumor model toward PD-1/PD-L1 blockade monotherapy.

The synergistic effect of apatinib and PD-1 mAb in PD-1 mAb-resistant tumors with high expression of VEGFA

Apatinib is a small-molecule inhibitor of VEGFR-2 and has demonstrated encouraging anti-angiogenic activity in tumors. We evaluated the efficacy of apatinib or PD-1 mAb alone or in combination to detect whether apatinib has a role in revising the resistance to PD-1/PD-L1 blockade in VEGFA-overexpressed tumors. As previously described, PD-1 mAb alone did not exhibit treatment efficacy in VEGFA-overexpressed tumors. Additionally, apatinib alone had mild influence on tumor growth, while the administration of apatinib plus PD-1 mAb notably inhibited tumor growth in CT26-VEGFA (Fig. 4a–d) and 4T1-VEGFA tumors (Fig. 4e–h). Tumor weight was 988.4 ± 592.1 mg (CT26) and 594.6 ± 197.7 mg (4T1), compared to the control group where the number was 4926.0 ± 1589.0 mg (CT26) and 2493.0 ± 324.4 mg (4T1) (Fig. 4d, h). Interestingly, it was found that unlike tumors overexpressing VEGFA, the tumor burden of monotherapy and combination therapy with apatinib or PD-1 mAb was remarkably reduced, much less than that of the control group in normal CT26-NC and 4T1-NC tumors. However, the anti-tumor advantage of the combination treatment group was not superior to the two single treatment groups. Namely, apatinib seemed to enhance the efficiency of PD-1 mAb only in VEGFA-overexpressed PD-1 mAb-resistant tumors.

The combination of apatinib and PD-1 mAb effectively optimized the angiogenesis microenvironment in hyperangiogenic, hypoxic and PD-1 mAb-resistant tumors

Apatinib was administrated prior to PD-1 mAb to create a better TME with reduced hyperangiogenesis and

immunosuppression. The assumption seemed to succeed based upon the following results. In both CT26-VEGFA and 4T1-VEGFA tumors, the expression of VEGFA and HIF-1 α was conspicuously reduced after the application of apatinib (Fig. 5a–c). Thus, angiogenesis and hypoxia had been notably improved when using apatinib. We also noticed a slight decrease of endothelial cell marker CD31 expression after apatinib treatment compared with the control group in CT26-VEGFA tumors. And no significant differences were observed between four different treatments of 4T1-VEGFA tumors (Fig. 5a, d). Together, it may suggest the main role of apatinib in vascular normalization.

Double-labeled immunofluorescent staining of VEGFA and HIF-1 α in CT26-VEGFA tumors is shown in Fig. 5e. Co-localization revealed a poor local circumstance of the tumor due to increased expression of VEGFA in tumor cells. The single drug of PD-1 mAb did not appear to be an effective method to alleviate local hyperangiogenesis and severe hypoxia. Nevertheless, both VEGFA and HIF-1 α expression showed an encouraging decline on account of apatinib. Thus, apatinib can normalize tumor vascular system and mitigate depressive angiogenesis and hypoxia by targeting VEGFA/VEGFR-2 signaling pathway and provide opportunities for the application of PD-1 mAb in hyperangiogenic, hypoxic and PD-1 mAb-resistant tumors.

The combination of apatinib and PD-1 mAb notably improved the immune microenvironment in hyperangiogenic, hypoxic and PD-1 mAb-resistant tumors

Though apatinib has been shown to alleviate the hyperangiogenesis and hypoxia, the tumor immune microenvironment, playing a quite pivotal role in the response to PD-1/PD-L1 blockade, still requires far more attention. The response to PD-1/PD-L1 blockade is usually associated with increased CD8⁺ T cell infiltration [5, 6], so we examined the number of effector CD8⁺ T cells by flow cytometry and immunohistochemistry. Combination of apatinib and PD-1 mAb showed an appreciable enhancement of effector cell infiltration, though CD8⁺ T cells were reduced to a certain extent in hyperangiogenic tumors, whereas PD-1 mAb monotherapy did not increase cell infiltration (Fig. 6a, c). We also evaluated the percentage of CD8⁺ T cell in spleen, and no similar difference were found (data not shown). Thus, it is indicated that the combining administration had a direct impact on tumor immune microenvironment rather than affecting peripheral immunity. As CD8⁺ T exhausted cells are major targets of immune checkpoint blockade, the exhaustion status of CD8⁺ T cells will limit the therapeutic potential [43]. PD-1 mAb alone had no effect on the expression of VEGFA-induced TOX-upregulation. However, apatinib

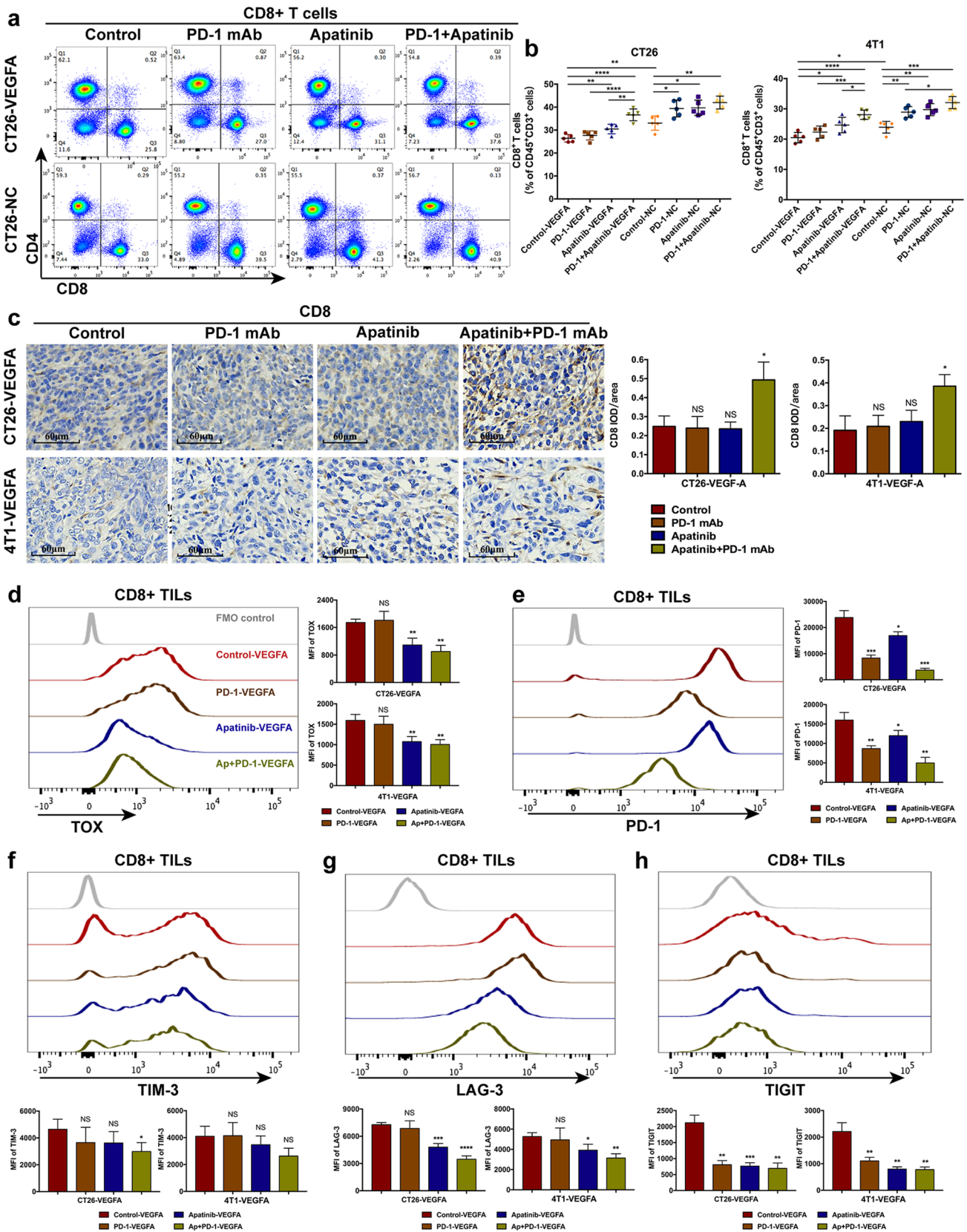


Fig. 6 Apatinib combined with PD-1 mAb increased CD8⁺ TILs cells and restored CD8⁺ T exhausted cells in PD-1 mAb resistant cancers. The ratio of CD8⁺ T cell subsets in T lymphocytes was determined by flow cytometry (a–b), **** $p < 0.0001$, *** $p < 0.001$, ** $p < 0.01$, * $p < 0.05$. Immunohistochemistry was also performed to show the expression of CD8 in hyperangiogenic, hypoxia and PD-1 mAb resistant tumors (c). The expression of TOX (a), PD-1 (e), TIM-3 (f), LAG-3 (g), TIGIT (h) among CD8⁺ TILs were examined to analyze the exhaustion status of CD8⁺ T cells, **** $p < 0.0001$, *** $p < 0.001$, ** $p < 0.01$, * $p < 0.05$. -VEGFA: the group of mice bearing VEGFA-overexpressed tumor cells, -NC: the group of mice bearing tumor cells with empty vector

notably reduced the level of TOX in CD8⁺ TILs (Fig. 6d). The combination of apatinib and PD-1 mAb also remarkably decreased the expression of PD-1, TIM-3, LAG-3 and TIGIT on CD8⁺ T cells (Fig. 6e, h). Hence, the combination therapy also reversed the exhaustion of CD8⁺ tumor-infiltrating T cells and possibly promoted the potential of immunotherapy.

Tregs, M2-like macrophages, and MDSCs, are important components in TME, and are often involved in the inhibition of anti-tumor activity. The ratio of these subsets tested through flow cytometry experienced a significant reduction, thereby resulting in a less suppressed immune microenvironment (Fig. 7a–e). A conspicuous increase in CD8⁺ T cells and a concomitant decrease in immunosuppressive cells, along with the down-regulation of T cell exhaustion status, suggested an enhancement of the anti-tumor immunity under the combination of apatinib and PD-1 mAb, which was in accordance with the variety of tumor burden.

In addition, we evaluated the tumor immunity using MCP-counter method. Though it is easy to recognize discrepancies between quantification of cell population by gene signatures expression and the density of the corresponding cell type in the tissue, MCP-counter scores was demonstrated to correlate strongly with the abundance of the corresponding population [44]. In hyperangiogenic mouse tumors, the expression level of immunity-related genes in the combination group was higher than that in the control group or PD-1 mAb group (Fig. 7f). The reinforcement of immune functioning in TME is likely to be associated with our combination treatment. And immunity-related gene levels in the combination group were not superior to the single administration in normal tumors. Therefore, apatinib in combination with PD-1 mAb could improve hyper-angiogenesis and -hypoxia, and induce supporting anti-tumor immunity in VEGFA-overexpressed PD-1 mAb-resistant tumors, which is considered as underlying mechanism to revise resistance to PD-1/PD-L1 blockade.

Discussion

The formation of tumor vessels is indispensable for tumor growth and metastasis. VEGFA, the critical and most active pro-angiogenic factor among the VEGF family, plays an

important role in the development of tumors. It is verified that high-level VEGFA is associated with poor prognosis in tumors including gastric cancer, ovarian cancer, hepatic carcinoma, NSCLC and endometrial cancer [45–49]. Using the data from TCGA, our study also identified that high-level VEGFA mRNA is correlated with significantly reduced survival in pan-cancer including breast cancer. An obvious separation of the survival curves in colon cancer was found, though there was no significant difference of survival between the VEGFA-high and VEGFA-low groups. Further analysis showed that microsatellite state might affect the role of VEGFA on prognosis, and high level of VEGFA is notably related to worse OS in MSS colon cancer. Consistent with previous studies, we found that upregulation of VEGFA expressively enhanced cell proliferation, migration and invasion in vitro [50, 51], and significantly accelerated tumor growth in mice. Thus, our results suggest that tumor cells tend to show increased malignancy with hyperexpression of VEGFA. On account of the evident VEGFA effect on pro-angiogenesis, sustained excessive VEGFA signal aggravates abnormal tumor vasculature, poor perfusion and insufficient oxygen supply. This, along with the positive feedback of HIF-1 α , forms the TME with hypoxia and hyperangiogenesis [11, 12]. Then, hypoxic, hyperangiogenic tumors regulate the microenvironment into an immunosuppressive one ultimately [52, 53]. Consistent with those studies, our study found serious hypoxia and abnormal angiogenesis, as well as repressed anti-tumor immunity in both human tumors and mouse tumor models with high expression of VEGFA.

PD-1/PD-L1 inhibitors are recognized to be functionless without the presence of effector T cells in tumor areas. Therefore, the hypoxic, hyperangiogenic and immunosuppressive TME caused by VEGFA overexpression is absolutely not conducive to the PD-1/PD-L1 blockade. In our study, single PD-1 mAb was administrated on tumors with and without high expression of VEGFA. Results showed that monotherapy PD-1 mAb remarkably inhibited tumor growth in mice bearing the tumor cells without VEGFA overexpression. On the contrary, there was no significant inhibition of tumor growth after PD-1 mAb applying in VEGFA-overexpressed tumor mouse models. Thus, the VEGFA-overexpressed mouse model established in our study, characterized by hyperangiogenic and hypoxic, immunosuppressive TME, showed innate resistance to PD-1/PD-L1 blockade.

We assume that improvement in the hypoxic and hyperangiogenic TME could be a potential strategy to overcome the VEGFA-related innate resistance. Conventional therapeutic agents always show killing effect on rapidly proliferating cancer cells; however, those agents do not directly target the hypoxia in TME. As a mutual cause/effect between hypoxia and abnormal tumor angiogenesis, a vicious circle then generates. Actually, single AA therapy has not brought long-term OS benefits, while increasing attention is being

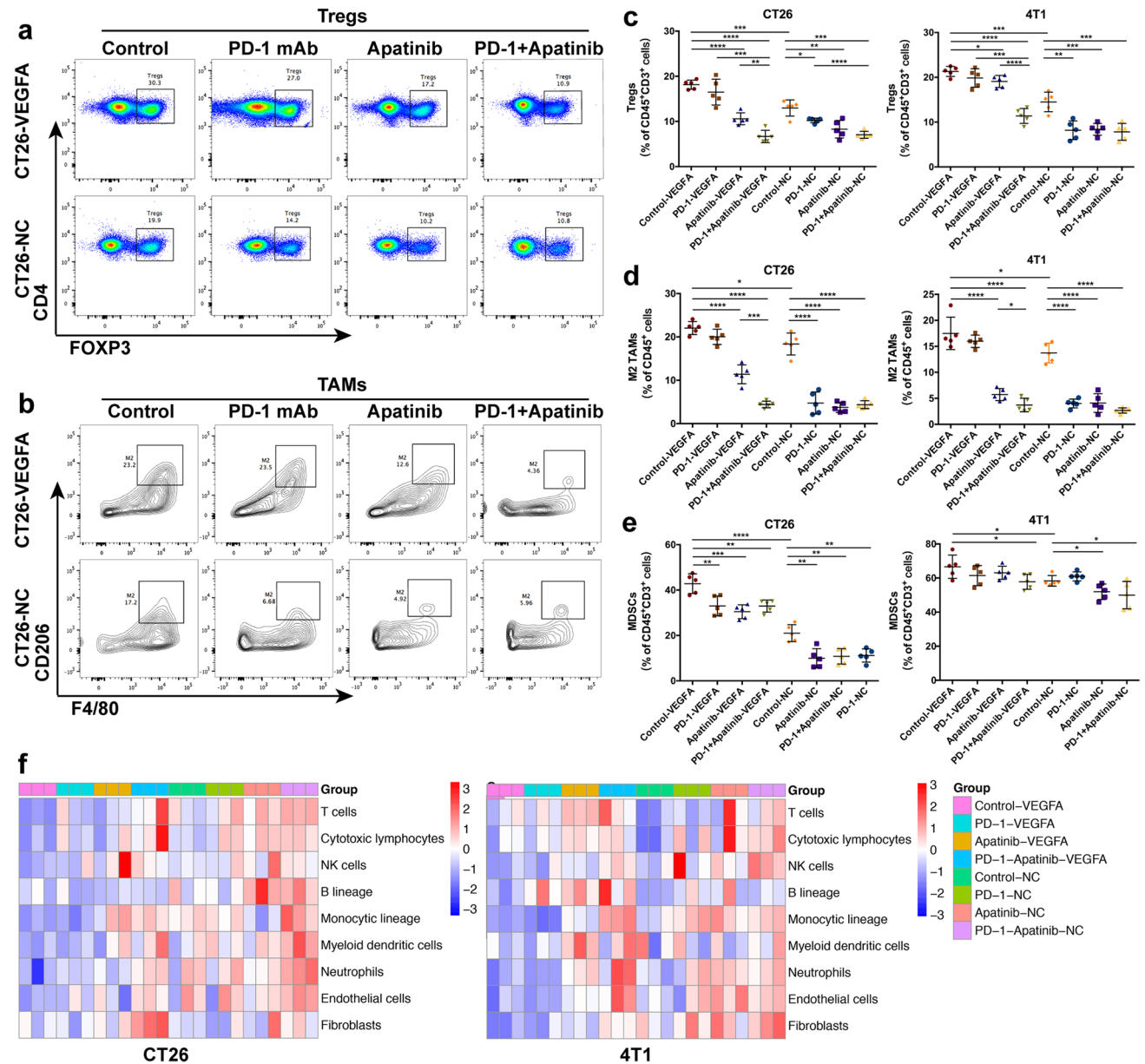


Fig. 7 Effects of the combination therapy of apatinib and PD-1 mAb on tumor immunomicroenvironment. The decreased ratio of Treg cell subsets in T lymphocytes of CT26 and 4T1 tumors (**a** and **c**). The variety of M2-like macrophages (**b** and **d**) and myeloid-derived suppressor cells (**e**) in immune cells in CT26 and 4T1 tumors,

**** $p < 0.0001$, *** $p < 0.001$, ** $p < 0.01$, * $p < 0.05$. **f** The heat map displayed the distinct expression of the genes associated with immune function in CT26 and 4T1, using MCP-counter scores. -VEGFA: the group of mice bearing VEGFA-overexpressed tumor cells, -NC: the group of mice bearing tumor cells with empty vector

attracted on its role of vascular normalization. Blocking VEGF signaling can increase the pericyte coverage and trim immature vessels to enhance vessel stabilization and reduce vascular leakiness, thereby alleviating hypoxia and improving penetration of drugs in tumors [54–56]. In our study, "vascular normalizing" appears to be more dominant in anti-tumor treatment with low-dose apatinib than "vessel pruning" due to slight differences in MVD after application of apatinib. Thus, it is observed that apatinib notably

inhibited hyperangiogenesis and improved hypoxia in PD-1 mAb innate resistant tumors with hypoxia, hyperangiogenesis and immunosuppression characteristics. These results demonstrated the potential for apatinib to normalize tumor vasculature. Likewise, cediranib is proved to transiently increase perfusion and oxygenation in newly diagnosed glioblastoma patients and associated with improved OS [57]. Similar findings on improved vascular function and

alleviation of hypoxia have been reported in NSCLC and breast cancer patients treated with bevacizumab [58, 59].

Originally, anti-angiogenesis agents were developed to interfere with neo-vascularization and starve tumor. Huang et al. [60] conducted a study to investigate the relationship between anti-angiogenesis dose and efficacy. The results demonstrated that lower dose of anti-angiogenesis agent was superior to higher dose treatment in inducing homogeneous tumor vessel normalization. Similarly, phase I study of ramucirumab plus pembrolizumab showed that higher doses of ramucirumab did not provide significantly improved clinical benefits [61]. A very high dose could cause rapid reduction in tumor perfusion and even aggravate hypoxia due to excessive pruning of tumor vessels [62]. Time of apatinib administration and dosage are worthy of much attention in the combination treatment. In our study, apatinib was administered before PD-1 mAb to act its role in vascular normalization and immune regulation, and a low dose was chosen. Retrospective study found that patients receiving ramucirumab before immune checkpoint therapy have longer OS than those treated with ramucirumab after the ICI therapy (31.4 m vs. 26.5 m) [23]. Studies demonstrating the efficacy of apatinib reveal that 100 mg/kg is a lower dose with efficacy [63, 64], much lower than 150 mg/kg, 200 mg/kg or even higher doses in other mouse models [65–67]. Thus, we chose 100 mg/kg as the dose of apatinib to maximize its benefits. However, the time window of vascular normalization induced by anti-angiogenesis agents is difficult to determine. Effective monitoring and earlier lines of the combination therapy may be more effective in human beings [61].

Normalization of tumor vasculature not only improves vascular function and alleviates hypoxia, but also has regulatory effect on anti-tumor immunity within TME. Preclinical studies showed that VEGF blockade and GM-CSF-secreting cancer immunotherapy can markedly increase CD8⁺ TILs and decrease suppressive Tregs in colon and melanoma mouse models [68]. Moreover, a recent study reported that VEGFA induces TOX upregulation to drive T cell exhaustion, which can be restored through dual blockade of PD-1 and VEGFA in MSS colon tumors [42]. Huang et al. [60] discovered in a breast cancer model that anti-VEGFR-2 antibodies (DC101), with adequate normalizing doses, could reprogram TME away from immunosuppression and enhance efficacy of immunotherapy. Analogously, the combination of antiangiogenesis and cytokine (IL-12 and GM-CSF) gene therapies induced high levels of cytotoxic cells and reduced the levels of immunosuppressive effectors in tumor regions, thus enhancing anti-tumor effects in hepatocellular cancer models [69]. Our study demonstrates that apatinib has the potential to reverse the immunosuppression in VEGFA-mediated, hyperangiogenic and hypoxic tumors. Encouragingly, combining apatinib with PD-1 mAb

increased CD8⁺ TILs, restored CD8⁺ T cell exhaustion and down-regulated co-expression of inhibitory receptors (PD-1, TIM-3, LAG-3 and TIGIT), and reduced accumulation of inhibitory immune cells including Tregs, M2-like TAMs and MDSCs. The heat map in Fig. 7 also suggests a strengthened immune microenvironment in PD-1 mAb-resistant mouse model with the combination therapy. The increased trafficking of CD8⁺ T cells and reversed CD8⁺ T exhausted cells is recognized as the main factor to facilitate the ICI to produce active anti-tumor effects. Simultaneously, the immunostimulatory TME, notably transformed from former immunosuppressive one, also promotes CD8⁺ T cell infiltration and serves as an assistance to immune therapy. Hence, consistent with these studies, antiangiogenic agents, especially apatinib targeting VEGFA/VEGFR-2 pathway, are proved to provide advantages of reducing tumor immune tolerance.

The IMpower150 trial assessed the combination of atezolizumab, bevacizumab, carboplatin and paclitaxel (ABCP) for previously untreated patients with metastatic, nonsquamous NSCLC. This pivotal phase III trial demonstrated an increase of 1.5 months in the median progression-free survival (PFS) and an increase of 4.5 months in the median OS for patients treated with ABCP when compared with the combination of bevacizumab, carboplatin and paclitaxel (BCP) [70]. Survival improvement was not observed in atezolizumab plus carboplatin plus paclitaxel (ACP) group versus in BCP one. The result of IMpower150 trial indicated remarkable synergistic effect of AA and ICI. Our study also illustrates that PD-1 mAb combined with apatinib has significant synergistic effect on inhibiting tumor growth in VEGFA-overexpressed, innate anti-PD-1 resistance mouse models. Judicious dosing of apatinib can normalize vasculature and modulate the tumor immunosuppressive microenvironment, and hence reverse PD-1/PD-L1 blockade resistance.

The resistance to PD-1/PD-L1 blockade can be ascribed to the variations in any aspect of the anti-tumor immunity cycle, such as inability to produce immunogenic neoantigens, invalid antigen processing, severe absence of infiltrating lymphocytes and enrichment of immunosuppressive components. Theoretically, AA and ICI combination therapy may benefit more for the patients with hyperangiogenic and hypoxic TME. Actually, this study finds that the ICI and AA combination therapy has no significant synergistic effect on tumors without VEGFA-overexpressed, hyperangiogenic and hypoxic TME. Data from patients with biliary tract cancer showed that ramucirumab plus pembrolizumab did not demonstrate an improvement in survival [28]. In some tumors including gastric cancer, gastroesophageal cancer and urothelial carcinoma, the ORR of AA and ICI combination therapy did not exceed 18% [61, 71]. In addition, the patients who received AA combined with ICI may experience more adverse effects

and financial burden. In the encouraging IMpower 150 trial, the incidence of grade 3–4 treatment-related adverse effect (TRAE) is up to 57% [70] in the ABCP group, and cost-effectiveness analysis in USA reported an ICER (incremental cost-effectiveness ratio) over \$500,000 per QALY (quality-adjusted life-year) [72]. In the CheckMate 016 trial of nivolumab in combination with sunitinib or pazopanib, 100% experienced a TRAE, and the incidence of grade 3–4 TRAE was as high as 82% or 70%, respectively [26]. In a phase III trial, adverse events of grade 3 or 4 occurred in 71.2% of the patients receiving avelumab plus axitinib, though PFS was significantly improved [24]. The avelumab and axitinib combination has also caused 58% TRAEs in patients with advanced clear-cell RCC [73]. Analysis showed that pembrolizumab plus axitinib is not cost-effective versus sunitinib for RCC patients in China [74]. Based on the above-mentioned, it may be reasonable to screen the most appropriate patients according to the hyper-angiogenic and hypoxic tumor microenvironment before the AA and ICI combination therapy, since the combination therapy not only has a synergistic anti-tumor effect but also is more toxic and costly compared with the monotherapy.

In general, our study successfully established an VEGFA-overexpressed, innate anti-PD-1 resistant mouse model in colon and breast cancer. It is demonstrated that prior blockade of VEGFA/VEGFR-2 signaling pathway using low-dose apatinib overcomes the innate resistance to PD-1/PD-L1 blockade and mediated synergistic anti-tumor response in VEGFA-overexpressed, hyperangiogenic and hypoxic tumors. TME characteristics should be prioritized in screening appropriate patients so as to administer AA and ICI combination therapy.

Acknowledgements We gratefully thank the Natural Science Foundation of China and School of Medicine, Shanghai Jiaotong University, for the funding.

Author contributions XW and WD designed and supervised the study. QHW performed the experiments in vitro. QHW and JZG established the animal model and conducted the animal study. JZG was responsible for the TCGA and mRNA sequencing analysis. QHW and XW completed the manuscript. All authors read and approved the final manuscript.

Funding This work is supported by grants from National Natural Science Foundation of China (81472843 to W. X.) and the study program of clinical capacity in urgently needed postgraduate majors in the School of Medicine, Shanghai Jiaotong University (JQ201703).

Compliance with ethical standards

Conflict of interest The authors declare that they have no competing interests.

Ethics approval We state that animal experiment in our study was approved by the Institutional Animal Care and Use Committee of Shanghai Jiao Tong University.

References

- Zou W, Wolchok JD, Chen L (2016) PD-L1 (B7–H1) and PD-1 pathway blockade for cancer therapy: Mechanisms, response biomarkers, and combinations. *Science translational medicine* 8(328):328rv324. <https://doi.org/10.1126/scitranslmed.aad71118>
- Abril-Rodriguez G, Ribas A (2017) SnapShot: immune checkpoint inhibitors. *Cancer Cell* 31(6):848–848.e841. <https://doi.org/10.1016/j.ccell.2017.05.010>
- Sharma P, Allison JP (2015) The future of immune checkpoint therapy. *Science* 348(6230):56–61. <https://doi.org/10.1126/science.aaa8172>
- Hodi FS, O'Day SJ, McDermott DF, Weber RW, Sosman JA, Haanen JB et al (2010) Improved survival with ipilimumab in patients with metastatic melanoma. *N Engl J Med* 363(8):711–723. <https://doi.org/10.1056/NEJMoa1003466>
- Topalian SL, Hodi FS, Brahmer JR, Gettinger SN, Smith DC, McDermott DF et al (2012) Safety, activity, and immune correlates of anti-PD-1 antibody in cancer. *N Engl J Med* 366(26):2443–2454. <https://doi.org/10.1056/NEJMoa1200690>
- Hamid O, Robert C, Daud A, Hodi FS, Hwu WJ, Kefford R et al (2013) Safety and tumor responses with lambrolizumab (anti-PD-1) in melanoma. *N Engl J Med* 369(2):134–144. <https://doi.org/10.1056/NEJMoa1305133>
- Wang Q, Wu X (2017) Primary and acquired resistance to PD-1/PD-L1 blockade in cancer treatment. *Int Immunopharmacol* 46:210–219. <https://doi.org/10.1016/j.intimp.2017.03.015>
- Hugo W, Zaretsky JM, Sun L, Song C, Moreno BH, Hu-Lieskova S et al (2016) Genomic and transcriptomic features of response to Anti-PD-1 therapy in metastatic melanoma. *Cell* 165(1):35–44. <https://doi.org/10.1016/j.cell.2016.02.065>
- Huang Y, Goel S, Duda DG, Fukumura D, Jain RK (2013) Vascular normalization as an emerging strategy to enhance cancer immunotherapy. *Cancer Res* 73(10):2943–2948. <https://doi.org/10.1158/0008-5472.can-12-4354>
- Maeda H, Wu J, Sawa T, Matsumura Y, Hori K (2000) Tumor vascular permeability and the EPR effect in macromolecular therapeutics: a review. *J Control Release* 65(1–2):271–284
- Viallard C, Larrivee B (2017) Tumor angiogenesis and vascular normalization: alternative therapeutic targets. *Angiogenesis* 20(4):409–426. <https://doi.org/10.1007/s10456-017-9562-9>
- Jain RK (2014) Antiangiogenesis strategies revisited: from starving tumors to alleviating hypoxia. *Cancer Cell* 26(5):605–622. <https://doi.org/10.1016/j.ccell.2014.10.006>
- Colegio OR, Chu NQ, Szabo AL, Chu T, Rhebergen AM, Jairam V et al (2014) Functional polarization of tumour-associated macrophages by tumour-derived lactic acid. *Nature* 513(7519):559–563. <https://doi.org/10.1038/nature13490>
- Curjel TJ, Coukos G, Zou L, Alvarez X, Cheng P, Mottram P et al (2004) Specific recruitment of regulatory T cells in ovarian carcinoma fosters immune privilege and predicts reduced survival. *Nat Med* 10(9):942–949. <https://doi.org/10.1038/nm1093>
- Noy R, Pollard JW (2014) Tumor-associated macrophages: from mechanisms to therapy. *Immunity* 41(1):49–61. <https://doi.org/10.1016/j.immuni.2014.06.010>
- Facciabene A, Peng X, Hagemann IS, Balint K, Barchetti A, Wang LP et al (2011) Tumour hypoxia promotes tolerance and

- angiogenesis via CCL28 and T(reg) cells. *Nature* 475(7355):226–230. <https://doi.org/10.1038/nature10169>
17. Gabrilovich D, Ishida T, Oyama T, Ran S, Kravtsov V, Nadaf S et al (1998) Vascular endothelial growth factor inhibits the development of dendritic cells and dramatically affects the differentiation of multiple hematopoietic lineages in vivo. *Blood* 92(11):4150–4166
 18. Terme M, Pernet S, Marcheteau E, Sandoval F, Benhamouda N, Colussi O et al (2013) VEGFA-VEGFR pathway blockade inhibits tumor-induced regulatory T-cell proliferation in colorectal cancer. *Can Res* 73(2):539–549. <https://doi.org/10.1158/0008-5472.can-12-2325>
 19. Palazón A, Aragonés J, Morales-Kastresana A, de Landázuri MO, Melero I (2012) Molecular pathways: hypoxia response in immune cells fighting or promoting cancer. *Clin Cancer Res* 18(5):1207–1213. <https://doi.org/10.1158/1078-0432.ccr-11-1591>
 20. Ohm JE, Gabrilovich DI, Sempowski GD, Kisseleva E, Parman KS, Nadaf S et al (2003) VEGF inhibits T-cell development and may contribute to tumor-induced immune suppression. *Blood* 101(12):4878–4886. <https://doi.org/10.1182/blood-2002-07-1956>
 21. Chen PL, Roh W, Reuben A, Cooper ZA, Spencer CN, Prieto PA et al (2016) Analysis of immune signatures in longitudinal tumor samples yields insight into biomarkers of response and mechanisms of resistance to immune checkpoint blockade. *Cancer Discov* 6(8):827–837. <https://doi.org/10.1158/2159-8290.cd-15-1545>
 22. McDermott DF, Huseni MA, Atkins MB, Motzer RJ, Rini BI, Escudier B et al (2018) Clinical activity and molecular correlates of response to atezolizumab alone or in combination with bevacizumab versus sunitinib in renal cell carcinoma. *Nat Med* 24(6):749–757. <https://doi.org/10.1038/s41591-018-0053-3>
 23. Molife C, Hess LM, Cui ZL, Li XI, Beyrer J, Mahoui M et al (2019) Sequential therapy with ramucirumab and/or checkpoint inhibitors for non-small-cell lung cancer in routine practice. *Future Oncol* 15(25):2915–2931. <https://doi.org/10.2217/fon-2018-0876>
 24. Motzer RJ, Penkov K, Haanen J, Rini B, Albiges L, Campbell MT et al (2019) Avelumab plus Axitinib versus Sunitinib for Advanced Renal-Cell Carcinoma. *N Engl J Med* 380(12):1103–1115. <https://doi.org/10.1056/NEJMoa1816047>
 25. Rini BI, Powles T, Atkins MB, Escudier B, McDermott DF, Suarez C et al (2019) Atezolizumab plus bevacizumab versus sunitinib in patients with previously untreated metastatic renal cell carcinoma (IMmotion151): a multicentre, open-label, phase 3, randomised controlled trial. *Lancet* 393(10189):2404–2415. [https://doi.org/10.1016/s0140-6736\(19\)30723-8](https://doi.org/10.1016/s0140-6736(19)30723-8)
 26. Amin A, Plimack ER, Ernstoff MS, Lewis LD, Bauer TM, McDermott DF et al (2018) Safety and efficacy of nivolumab in combination with sunitinib or pazopanib in advanced or metastatic renal cell carcinoma: the CheckMate 016 study. *J Immunother Cancer* 6(1):109. <https://doi.org/10.1186/s40425-018-0420-0>
 27. Makker V, Rasco D, Vogelzang NJ, Brose MS, Cohn AL, Mier J et al (2019) Lenvatinib plus pembrolizumab in patients with advanced endometrial cancer: an interim analysis of a multicentre, open-label, single-arm, phase 2 trial. *Lancet Oncol* 20(5):711–718. [https://doi.org/10.1016/s1470-2045\(19\)30020-8](https://doi.org/10.1016/s1470-2045(19)30020-8)
 28. Arkenau HT, Martin-Liberal J, Calvo E, Penel N, Krebs MG, Herbst RS et al (2018) Ramucirumab plus pembrolizumab in patients with previously treated advanced or metastatic biliary tract cancer: nonrandomized, open-label, phase I trial (JVDF). *Oncologist* 23(12):1407–e1136. <https://doi.org/10.1634/theoncologist.2018-0044>
 29. Li J, Zhao X, Chen L, Guo H, Lv F, Jia K et al (2010) Safety and pharmacokinetics of novel selective vascular endothelial growth factor receptor-2 inhibitor YN968D1 in patients with advanced malignancies. *BMC Cancer* 10:529. <https://doi.org/10.1186/1471-2407-10-529>
 30. Fang S, Zhang M, Wei G, Lu KH (2018) Apatinib as a third- or further- line treatment in patients with advanced NSCLC harboring wild-type EGFR. *Oncotarget* 9(6):7175–7181. <https://doi.org/10.18632/oncotarget.23612>
 31. Hu X, Zhang J, Xu B, Jiang Z, Ragaz J, Tong Z et al (2014) Multicenter phase II study of apatinib, a novel VEGFR inhibitor in heavily pretreated patients with metastatic triple-negative breast cancer. *Int J Cancer* 135(8):1961–1969. <https://doi.org/10.1002/ijc.28829>
 32. Kong Y, Sun L, Hou Z, Zhang Y, Chen P, Cui Y et al (2017) Apatinib is effective for treatment of advanced hepatocellular carcinoma. *Oncotarget* 8(62):105596–105605. <https://doi.org/10.18632/oncotarget.22337>
 33. Li F, Liao Z, Zhang C, Zhao J, Xing R, Teng S et al (2018) Apatinib as targeted therapy for sarcoma. *Oncotarget* 9(36):24548–24560. <https://doi.org/10.18632/oncotarget.24647>
 34. Lin Y, Wang C, Gao W, Cui R, Liang J (2017) Overwhelming rapid metabolic and structural response to apatinib in radioiodine refractory differentiated thyroid cancer. *Oncotarget* 8(26):42252–42261. <https://doi.org/10.18632/oncotarget.15036>
 35. Miao M, Deng G, Luo S, Zhou J, Chen L, Yang J et al (2018) A phase II study of apatinib in patients with recurrent epithelial ovarian cancer. *Gynecol Oncol* 148(2):286–290
 36. Bindea G, Mlecnik B, Tosolini M, Kirilovsky A, Waldner M, Obenauf AC et al (2013) Spatiotemporal dynamics of intratumoral immune cells reveal the immune landscape in human cancer. *Immunity* 39(4):782–795. <https://doi.org/10.1016/j.immuni.2013.10.003>
 37. Becht E, Giraldo NA, Lacroix L, Buttard B, Elarouci N, Petitprez F et al (2016) Estimating the population abundance of tissue-infiltrating immune and stromal cell populations using gene expression. *Genome Biol* 17(1):218. <https://doi.org/10.1186/s13059-016-1070-5>
 38. Aslakson CJ, Miller FR (1992) Selective events in the metastatic process defined by analysis of the sequential dissemination of subpopulations of a mouse mammary tumor. *Can Res* 52(6):1399–1405
 39. Corbett TH, Griswold DP Jr, Roberts BJ, Peckham JC, Schabel FM Jr (1975) Tumor induction relationships in development of transplantable cancers of the colon in mice for chemotherapy assays, with a note on carcinogen structure. *Can Res* 35(9):2434–2439
 40. Alfei F, Kanev K, Hofmann M, Wu M, Ghoneim HE, Roelli P et al (2019) TOX reinforces the phenotype and longevity of exhausted T cells in chronic viral infection. *Nature* 571(7764):265–269. <https://doi.org/10.1038/s41586-019-1326-9>
 41. Khan O, Giles JR, McDonald S, Manne S, Ngiow SF, Patel KP et al (2019) TOX transcriptionally and epigenetically programs CD8(+) T cell exhaustion. *Nature* 571(7764):211–218. <https://doi.org/10.1038/s41586-019-1325-x>
 42. Kim CG, Jang M, Kim Y, Leem G, Kim KH, Lee H et al (2019) VEGF-A drives TOX-dependent T cell exhaustion in anti-PD-1-resistant microsatellite stable colorectal cancers. *Sci Immunol*. <https://doi.org/10.1126/sciimmunol.aay0555>
 43. Wherry EJ (2011) T cell exhaustion. *Nat Immunol* 12(6):492–499. <https://doi.org/10.1038/ni.2035>
 44. Petitprez F, Vano YA, Becht E, Giraldo NA, de Reynies A, Sautes-Fridman C et al (2018) Transcriptomic analysis of the tumor microenvironment to guide prognosis and immunotherapies. *Cancer Immunol Immunother C: II* 67(6):981–988. <https://doi.org/10.1007/s00262-017-2058-z>
 45. Guo LY, Zhu P, Jin XP (2016) Association between the expression of HIF-1 α and VEGF and prognostic implications in primary liver cancer. *Genet Mol Res*. <https://doi.org/10.4238/gmr.15028107>

46. Jantus-Lewintre E, Sanmartin E, Sirera R, Blasco A, Sanchez JJ, Taron M et al (2011) Combined VEGF-A and VEGFR-2 concentrations in plasma: diagnostic and prognostic implications in patients with advanced NSCLC. *Lung Cancer* 74(2):326–331. <https://doi.org/10.1016/j.lungcan.2011.02.016>
47. Wang J, Taylor A, Showell R, Trivedi P, Horimoto Y, Bagwan I et al (2014) Expression profiling and significance of VEGF-A, VEGFR2, VEGFR3 and related proteins in endometrial carcinoma. *Cytokine* 68(2):94–100. <https://doi.org/10.1016/j.cyto.2014.04.005>
48. Wang X, Chen X, Fang J, Yang C (2013) Overexpression of both VEGF-A and VEGF-C in gastric cancer correlates with prognosis, and silencing of both is effective to inhibit cancer growth. *Int J Clin Exp Pathol* 6(4):586–597
49. Yamamoto S, Konishi I, Mandai M, Kuroda H, Komatsu T, Nanbu K et al (1997) Expression of vascular endothelial growth factor (VEGF) in epithelial ovarian neoplasms: correlation with clinicopathology and patient survival, and analysis of serum VEGF levels. *Br J Cancer* 76(9):1221–1227
50. Xiao K, Ouyang Z, Tang HH (2018) Inhibiting the proliferation and metastasis of hilar cholangiocarcinoma cells by blocking the expression of vascular endothelial growth factor with small interfering RNA. *Oncol Lett* 16(2):1841–1848. <https://doi.org/10.3892/ol.2018.8840>
51. Zeng FC, Zeng MQ, Huang L, Li YL, Gao BM, Chen JJ et al (2016) Downregulation of VEGFA inhibits proliferation, promotes apoptosis, and suppresses migration and invasion of renal clear cell carcinoma. *Onco Targets Ther* 9:2131–2141. <https://doi.org/10.2147/ott.s98002>
52. Bergers G, Hanahan D (2008) Modes of resistance to antiangiogenic therapy. *Nat Rev Cancer* 8(8):592–603. <https://doi.org/10.1038/nrc2442>
53. Movahedi K, Laoui D, Gysemans C, Baeten M, Stange G, Van den Bossche J et al (2010) Different tumor microenvironments contain functionally distinct subsets of macrophages derived from Ly6C(high) monocytes. *Can Res* 70(14):5728–5739. <https://doi.org/10.1158/0008-5472.can-09-4672>
54. Cooke VG, LeBleu VS, Keskin D, Khan Z, O'Connell JT, Teng Y et al (2012) Pericyte depletion results in hypoxia-associated epithelial-to-mesenchymal transition and metastasis mediated by met signaling pathway. *Cancer Cell* 21(1):66–81. <https://doi.org/10.1016/j.ccr.2011.11.024>
55. Jain RK (2005) Normalization of tumor vasculature: an emerging concept in antiangiogenic therapy. *Science* 307(5706):58–62. <https://doi.org/10.1126/science.1104819>
56. Meng MB, Zaorsky NG, Deng L, Wang HH, Chao J, Zhao LJ et al (2015) Pericytes: a double-edged sword in cancer therapy. *Future Oncol* 11(1):169–179. <https://doi.org/10.2217/fo.14.123>
57. Batchelor TT, Gerstner ER, Emblem KE, Duda DG, Kalpathy-Cramer J, Snuderl M et al (2013) Improved tumor oxygenation and survival in glioblastoma patients who show increased blood perfusion after cediranib and chemoradiation. *Proc Natl Acad Sci USA* 110(47):19059–19064. <https://doi.org/10.1073/pnas.1318022110>
58. Heist RS, Duda DG, Sahani DV, Ancukiewicz M, Fidias P, Sequist LV et al (2015) Improved tumor vascularization after anti-VEGF therapy with carboplatin and nab-paclitaxel associates with survival in lung cancer. *Proc Natl Acad Sci USA* 112(5):1547–1552. <https://doi.org/10.1073/pnas.1424024112>
59. Tolane SM, Boucher Y, Duda DG, Martin JD, Seano G, Ancukiewicz M et al (2015) Role of vascular density and normalization in response to neoadjuvant bevacizumab and chemotherapy in breast cancer patients. *Proc Natl Acad Sci USA* 112(46):14325–14330. <https://doi.org/10.1073/pnas.1518808112>
60. Huang Y, Yuan J, Righi E, Kamoun WS, Ancukiewicz M, Neziyar J et al (2012) Vascular normalizing doses of antiangiogenic treatment reprogram the immunosuppressive tumor microenvironment and enhance immunotherapy. *Proc Natl Acad Sci USA* 109(43):17561–17566. <https://doi.org/10.1073/pnas.1215397109>
61. Herbst RS, Arkenau HT, Santana-Davila R, Calvo E, Paz-Ares L, Cassier PA et al (2019) Ramucicromab plus pembrolizumab in patients with previously treated advanced non-small-cell lung cancer, gastro-oesophageal cancer, or urothelial carcinomas (JVDF): a multicohort, non-randomised, open-label, phase 1a/b trial. *Lancet Oncol* 20(8):1109–1123. [https://doi.org/10.1016/s1470-2045\(19\)30458-9](https://doi.org/10.1016/s1470-2045(19)30458-9)
62. Chung AS, Kowanetz M, Wu X, Zhuang G, Ngu H, Finkle D et al (2012) Differential drug class-specific metastatic effects following treatment with a panel of angiogenesis inhibitors. *J Pathol* 227(4):404–416. <https://doi.org/10.1002/path.4052>
63. Wu S, Zhou J, Guo J, Hua Z, Li J, Wang Z (2019) Apatinib inhibits tumor growth and angiogenesis in PNET models. *Endocr Connect* 8(1):8–19. <https://doi.org/10.1530/ec-18-0397>
64. Tian S, Quan H, Xie C, Guo H, Lu F, Xu Y et al (2011) YN968D1 is a novel and selective inhibitor of vascular endothelial growth factor receptor-2 tyrosine kinase with potent activity in vitro and in vivo. *Cancer Sci* 102(7):1374–1380. <https://doi.org/10.1111/j.1349-7006.2011.01939.x>
65. Peng QX, Han YW, Zhang YL, Hu J, Fan J, Fu SZ et al (2017) Apatinib inhibits VEGFR-2 and angiogenesis in an in vivo murine model of nasopharyngeal carcinoma. *Oncotarget* 8(32):52813–52822. <https://doi.org/10.18632/oncotarget.17264>
66. Zhou K, Zhang JW, Wang QZ, Liu WY, Liu JL, Yao L et al (2019) Apatinib, a selective VEGFR2 inhibitor, improves the delivery of chemotherapeutic agents to tumors by normalizing tumor vessels in LoVo colon cancer xenograft mice. *Acta Pharmacol Sin* 40(4):556–562. <https://doi.org/10.1038/s41401-018-0058-y>
67. Liu ZJ, Zhou YJ, Ding RL, Xie F, Fu SZ, Wu JB et al (2018) In vitro and in vivo apatinib inhibits vasculogenic mimicry in melanoma MUM-2B cells. *PLoS ONE* 13(7):e0200845. <https://doi.org/10.1371/journal.pone.0200845>
68. Li B, Lalani AS, Harding TC, Luan B, Koprivnikar K, Huan TuG et al (2006) Vascular endothelial growth factor blockade reduces intratumoral regulatory T cells and enhances the efficacy of a GM-CSF-secreting cancer immunotherapy. *Clin Cancer Res Off J Am Assoc Cancer Res* 12(22):6808–6816. <https://doi.org/10.1158/1078-0432.ccr-06-1558>
69. Huang KW, Wu HL, Lin HL, Liang PC, Chen PJ, Chen SH et al (2010) Combining antiangiogenic therapy with immunotherapy exerts better therapeutic effects on large tumors in a woodchuck hepatoma model. *Proc Natl Acad Sci USA* 107(33):14769–14774. <https://doi.org/10.1073/pnas.1009534107>
70. Reck M, Mok TSK, Nishio M, Jotte RM, Cappuzzo F, Orlandi F et al (2019) Atezolizumab plus bevacizumab and chemotherapy in non-small-cell lung cancer (IMpower150): key subgroup analyses of patients with EGFR mutations or baseline liver metastases in a randomised, open-label phase 3 trial. *Lancet Respir Med* 7(5):387–401. [https://doi.org/10.1016/s2213-2600\(19\)30084-0](https://doi.org/10.1016/s2213-2600(19)30084-0)
71. Xu J, Zhang Y, Jia R, Yue C, Chang L, Liu R et al (2019) Anti-PD-1 antibody SHR-1210 combined with apatinib for advanced hepatocellular carcinoma, gastric, or esophagogastric junction cancer: an open-label, dose escalation and expansion study. *Clin Cancer Res Off J Am Assoc Cancer Res* 25(2):515–523. <https://doi.org/10.1158/1078-0432.ccr-18-2484>
72. Wan X, Luo X, Tan C, Zeng X, Zhang Y, Peng L (2019) First-line atezolizumab in addition to bevacizumab plus chemotherapy for metastatic, nonsquamous non-small cell lung cancer: a United States-based cost-effectiveness analysis. *Cancer*. <https://doi.org/10.1002/cncr.32368>

73. Choueiri TK, Larkin J, Oya M, Thistlethwaite F, Martignoni M, Nathan P et al (2018) Preliminary results for avelumab plus axitinib as first-line therapy in patients with advanced clear-cell renal-cell carcinoma (JAVELIN Renal 100): an open-label, dose-finding and dose-expansion, phase 1b trial. *Lancet Oncol* 19(4):451–460. [https://doi.org/10.1016/s1470-2045\(18\)30107-4](https://doi.org/10.1016/s1470-2045(18)30107-4)
74. Chen J, Hu G, Chen Z, Wan X, Tan C, Zeng X et al (2019) Cost-effectiveness analysis of pembrolizumab plus axitinib versus

sunitinib in first-line advanced renal cell carcinoma in China. *Clin Drug Investig*. <https://doi.org/10.1007/s40261-019-00820-6>

Publisher's Note Springer Nature remains neutral with regard to jurisdictional claims in published maps and institutional affiliations.